Mutual Inductance Modeling for Multiple *RLC* Interconnects with Application to Shield Insertion

Junmou Zhang and Eby G. Friedman

Department of Electrical and Computer Engineering
University of Rochester
Rochester, New York 14627–0231

***Abstract*— An effective mutual inductance is proposed in this paper to efficiently describe the inductive interactions among coupled signal lines. An efficient estimate of the crosstalk noise among multiple coupled *RLC* interconnects is achieved by simplifying the system of coupled lines into only two coupled *RLC* interconnects. The concept of an effective mutual inductance is further applied to a shielding technique, providing guidelines for inserting shields to reduce crosstalk noise in the presence of both capacitive and inductive coupling.**

I. Introduction

On-chip interconnect delay and crosstalk have become primary bottlenecks in determining the performance and signal integrity of deep submicrometer VLSI circuits. With faster signal rise times and lower resistance, the long wide wires in the upper metal layers can exhibit significant inductive effects. An efficient *RLC* model of the on-chip interconnect is therefore critical in high level design, logic synthesis, and physical design.

While capacitive coupling between non-adjacent wires can often be ignored and is primarily a nearest neighbor phenomenon [1], mutual inductive coupling is a long range issue and cannot be ignored in non-adjacent wires. The mutual inductance decays slowly with greater spacing and depends on the distribution of the induced currents. The return paths of the induced current often cannot be determined *a priori* in complex integrated circuits. With the assumption of current returning at infinity, Partial Element Equivalent Circuit (PEEC) models can be directly applied to circuit simulators like SPICE, obviating the need for knowing the distribution of the returned currents. A full matrix which includes the mutual inductances between all pairs of wires is necessary in the PEEC method to correctly model an *RLC* line, generating a dense partial inductance matrix. This dense partial inductance matrix, together with resistance and capacitance models, requires significant computational time and is an extremely difficult IC design and verification task. An approach to tackle this problem is to use an effective loop inductance to model high speed interconnects [2]. While the effective loop inductance efficiently describes the inductive characteristics of a single wire, it does not address the problem of crosstalk noise in a victim line induced by an aggressor signal.

An estimate of crosstalk noise among multiple *RLC* interconnects is required to implement efficient shielding techniques. Shield insertion is an effective method to reduce crosstalk noise and signal delay uncertainty, and has become common practice when routing critical signal and clock lines [3]. Inserting shield lines can greatly reduce capacitive coupling [1], and reduce the mutual inductive coupling by providing a closer current return path for both the aggressor and victim lines. Far reaching inductive coupling, however, cannot be completely eliminated, and can produce substantial crosstalk noise on a quiescent victim line. An efficient estimate of the crosstalk noise between coupled interconnects including the effects of shield insertion is therefore critical during the routing and verification phase to guarantee signal integrity. Guidelines are required to determine when a shield line should be inserted and whether a one sided shield or two sided shield is appropriate.

An effective mutual inductance is proposed in this paper to solve the problem of crosstalk noise among multiple coupled *RLC* interconnects and to provide guidelines for shield insertion. By converting coupled interconnects with multiple ground return lines into two coupled interconnects with an effective loop inductance and mutual inductance, an estimate of the crosstalk noise can be analytically determined [4]. Based on the effective mutual inductance and crosstalk noise models, the effect of shield insertion on reducing crosstalk noise in the presence of capacitive and inductive coupling is discussed in this paper.

The rest of the paper is organized as follows. In Section II, the concept of an effective mutual inductance is proposed to efficiently characterize the inductive interactions among multiple coupled *RLC* interconnects, and is applied to estimate crosstalk noise in an example structure composed of four couple *RLC* interconnects with varying separation. Based on the effective mutual inductance and crosstalk noise models, the effect of shield insertion on reducing crosstalk noise and guidelines for shield insertion in the presence of capacitive and inductive coupling are presented in Section III. Some conclusions are offered in Section IV.

II. Effective Mutual Inductance

Due to the presence of long range inductive coupling, crosstalk generally involves multiple coupled *RLC* interconnects. The effective loop inductance [2] is commonly used to avoid the complexity of the PEEC method. While the effective loop inductance is efficient in estimating the delay of the signal line, it does not address the issue of crosstalk noise caused by inductive coupling between an aggressor line and a victim line. In order to address crosstalk noise among multiple coupled *RLC* interconnects, the ground current return path of the inductances is first discussed in this section, followed by an introduction of the concept of an effective mutual inductance to efficiently characterize inductive coupling between an aggressor line and a victim line. Based on the effective mutual inductance, multiple coupled *RLC* interconnects can be modeled by two coupled signal lines, permitting an efficient estimate of the crosstalk noise. An example structure composed of four coupled *RLC* interconnects is presented to demonstrate the process for estimating crosstalk noise with the model described in [4].

Current in general is distributed among multiple return paths so as to minimize the total impendence $Z(\omega) = R + j\omega L$. At low

This research is supported in part by the Semiconductor Research Corporation under Contract No. 2003-TJ-1068, the DARPA/ITO under AFRL Contract F29601-00-K-0182, the National Science Foundation under contract No. CCR-0304574, the Fulbright Program under Grant # 87481764, grants from the New York State Office of Science, Technology & Academic Research to the Center for Advanced Technology - Electronic Imaging Systems and to the Microelectronics Design Center, and by grants from Xerox Corporation, IBM Corporation, Intel Corporation, Lucent Technologies Corporation, and Eastman Kodak Company.

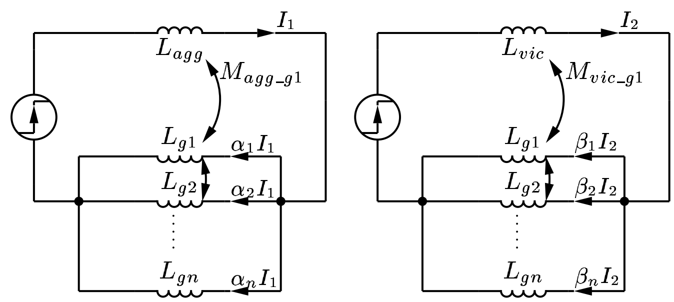

(a) Ground return current distribution for aggressor line

(b) Ground return current distribution for victim line

Fig. 1. Circuit models to determine the distribution of the ground return current for an aggressor line and a victim line

frequencies ($R >> j\omega L$), the line impedance and related return paths are dominated by the resistance. The return current, therefore, seeks the minimum resistance path, which can spread widely to multiple power or ground wires. At high frequencies ($R << j\omega L$), where the inductance dominates, the return current seeks the paths of least inductance. Since the line width of the power grid is much larger than the width of the signal lines, the return paths are commonly assumed to be confined to the closest power or ground lines [5]. In order to reduce interconnect delay, the global signal lines in the upper layer are made wider with less resistance. As a consequence, the inductive impedance of these wires is much greater than the resistive impedance, and the returned current seeks those paths that minimize the loop inductance.

Assuming the current only returns through the power and shield lines, the distribution of the ground return current of both the aggressor line and victim line can be determined by solving the branch currents for the circuits shown in Figs. 1(a) and 1(b). The inductances shown in Fig. 1 are partial inductances, and can be analytically determined [6] by

$$L_s = 0.0002l[ln(\frac{2l}{w+t}) + 0.5 - ln(\lambda)]\,, \tag{1}$$

$$M = 0.0002l[ln(\frac{l}{d} + \sqrt{1+\frac{l^2}{d^2}}) - \sqrt{1+\frac{d^2}{l^2}} + \frac{d}{l}]\,, \tag{2}$$

where l, w, and t are the length, width, and thickness of the interconnects, respectively, d is the separation between two interconnects, and $ln(\lambda)$ is only a function of the t/w ratio and is small as compared to the other terms (varying from 0 to 0.0025).

Applying a mesh analysis to the circuit with n ground lines as shown in Fig. 1(a), the branch current of each ground line $\mathbf{I}_b = [\alpha_1, \alpha_2, \ldots, \alpha_n]^T I_1$ can be obtained by solving [7],

$$\mathcal{L}\boldsymbol{\alpha} = 1\,, \tag{3}$$

$$\mathcal{L}_{ij} = L_{i,j} + L_{agg} - L_{i,agg} - L_{agg,j}\,. \tag{4}$$

The signs of α_i (i=1, 2, ..., n) are chosen to be negative to denote the inverse current direction and normalized to satisfy

$$-1 < \alpha_i < 0\,, \tag{5}$$

$$\sum_{i=1}^{n} \alpha_i = -1\,. \tag{6}$$

The branch current $\boldsymbol{\alpha}^T I_1$ can be further extended to include the aggressor line and victim line as $\boldsymbol{\alpha} = [1, 0, \alpha_1, \alpha_2, \ldots, \alpha_n]^T$. Similarly, the branch current for a victim line can be obtained as $\boldsymbol{\beta} = [0, 1, \beta_1, \beta_2, \ldots, \beta_n]^T$ by solving the circuit equations developed in Fig. 1(b).

As illustrated in Fig. 2, the inductive interactions within two signal lines and the surrounding ground lines can be incorporated into two coupled signal lines with effective loop inductances and an effective mutual inductance, permitting an estimate of the crosstalk noise between two lines. Assuming the current flowing through the

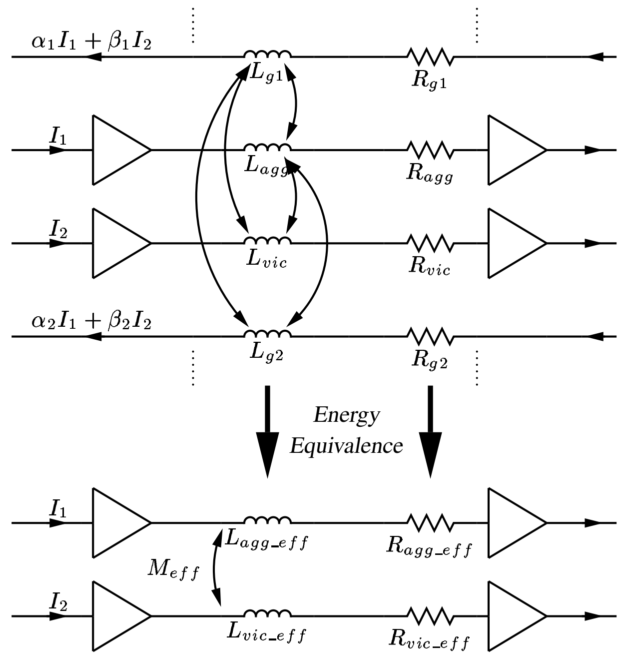

Fig. 2. Simplification of multiple interconnects into two coupled signal lines with effective loop inductances, effective mutual inductance, and effective resistances based on the equivalence of the magnetic energy stored in these two systems.

aggressor line is I_1 and the current through the victim line is I_2, the magnetic field energy stored in the original system is

$$\begin{aligned} W_m &= \frac{1}{2}\mathbf{I}_b^T \mathbf{L} \mathbf{I}_b\,, \\ &= \frac{1}{2}(\boldsymbol{\alpha} I_1 + \boldsymbol{\beta} I_2)^T \mathbf{L} (\boldsymbol{\alpha} I_1 + \boldsymbol{\beta} I_2)\,, \\ &= \frac{1}{2}\boldsymbol{\alpha}^T \mathbf{L} \boldsymbol{\alpha} I_1^2 + \frac{1}{2}\boldsymbol{\beta}^T \mathbf{L} \boldsymbol{\beta} I_2^2 \\ &\quad + \frac{1}{2}(\boldsymbol{\alpha}^T \mathbf{L} \boldsymbol{\beta} + \boldsymbol{\beta}^T \mathbf{L} \boldsymbol{\alpha}) I_1 I_2\,. \end{aligned} \tag{7}$$

The magnetic field energy stored in the equivalent system is

$$\begin{aligned} W'_m &= \frac{1}{2}\,[\,I_1 \;\; I_2\,] \begin{bmatrix} L_{agg\_eff} & M_{eff} \\ M_{eff} & L_{vic\_eff} \end{bmatrix} \begin{bmatrix} I_1 \\ I_2 \end{bmatrix}\,, \\ &= \frac{1}{2} L_{agg\_eff} I_1^2 + \frac{1}{2} L_{vic\_eff} I_2^2 + M_{eff} I_1 I_2\,. \end{aligned} \tag{8}$$

By using the equivalence of the magnetic energy stored in these two systems $W_m = W'_m$, the effective loop inductance and the effective mutual inductance are

$$L_{agg\_eff} = \boldsymbol{\alpha}^T \mathbf{L} \boldsymbol{\alpha}\,, \tag{9}$$

$$L_{vic\_eff} = \boldsymbol{\beta}^T \mathbf{L} \boldsymbol{\beta}\,, \tag{10}$$

$$M_{eff} = \frac{1}{2}(\boldsymbol{\alpha}^T \mathbf{L} \boldsymbol{\beta} + \boldsymbol{\beta}^T \mathbf{L} \boldsymbol{\alpha})\,. \tag{11}$$

Since $\boldsymbol{\alpha}^T \mathbf{L} \boldsymbol{\beta}$ is a number rather than a matrix, $\boldsymbol{\alpha}^T \mathbf{L} \boldsymbol{\beta} = (\boldsymbol{\alpha}^T \mathbf{L} \boldsymbol{\beta})^T = \boldsymbol{\beta}^T \mathbf{L}^T \boldsymbol{\alpha} = \boldsymbol{\beta}^T \mathbf{L} \boldsymbol{\alpha}$. The final step is valid because the partial inductance matrix $\mathbf{L}$ is symmetric. The effective mutual inductance in (11), therefore, can be further simplified to

$$M_{eff} = \boldsymbol{\alpha}^T \mathbf{L} \boldsymbol{\beta}. \tag{12}$$

The effective resistance can be determined from the equivalence of the power consumed in these two systems, as shown in (13) and (14), where $\boldsymbol{\alpha}$ and $\boldsymbol{\beta}$ include the aggressor line, victim line, and n ground return lines.

$$R_{agg\_eff} = \sum_{i=1}^{n+2} \alpha_i^2 R_i\,, \tag{13}$$

$$R_{vic\_eff} = \sum_{i=1}^{n+2} \beta_i^2 R_i\,. \tag{14}$$

The effective mutual inductance together with the crosstalk noise model described in [4] can be applied to analytically estimate the crosstalk noise among multiple coupled *RLC* interconnects. As an example, a four coupled *RLC* interconnect structure with a length of 3000 μm, as shown in Fig. 3, is used to compare the estimate of crosstalk noise, determined analytically through the effective mutual inductance, with SPICE.

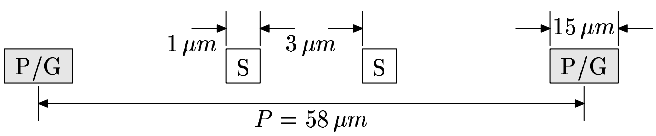

Fig. 3. An example structure of four coupled interconnects to present the concept of an effective mutual inductance

The partial inductance matrix extracted from the interconnect structure shown in Fig. 3 and the calculated effective loop inductances and effective mutual inductance are (units in nH)

$$\mathbf{L}_{partial} = \begin{bmatrix} 3.83745 & 2.65537 & 2.57137 & 2.19834 \\ 2.65537 & 4.96893 & 3.78485 & 2.57137 \\ 2.57137 & 3.78485 & 4.96893 & 2.65537 \\ 2.19834 & 2.57137 & 2.65537 & 3.83745 \end{bmatrix}, \tag{15}$$

$$\mathbf{L}_{effective} = \begin{bmatrix} 2.75793 & 1.57815 \\ 1.57816 & 2.75793 \end{bmatrix}. \tag{16}$$

The interconnect structure is simulated using FastHenry at a frequency of 10 GHz. The resulting loop inductance matrix is

$$\mathbf{L}_{fasthenry} = \begin{bmatrix} 2.75793 & 1.57817 \\ 1.57817 & 2.75793 \end{bmatrix}. \tag{17}$$

The effective loop inductances and the effective mutual inductance obtained from (9) - (12) are essentially the same as the simulation results developed from FastHenry [8], validating the method of effective mutual inductance, as shown in (16) and (17).

To estimate the crosstalk noise with a step input at the aggressor line, the capacitance matrix of the structure is extracted using OEA tools [9], and is (units in pF)

$$\mathbf{C} = \begin{bmatrix} 0.42409 & 0.00976 & 0.00175 & 0.00096 \\ 0.00976 & 0.10403 & 0.07885 & 0.00175 \\ 0.00175 & 0.07885 & 0.10403 & 0.00976 \\ 0.00096 & 0.00175 & 0.00976 & 0.42409 \end{bmatrix}. \tag{18}$$

The effective ground capacitances of the signal lines are determined by adding the coupling capacitance to the ground line to the ground capacitance, yielding the effective capacitance matrix,

$$\mathbf{C}_{effective} = \begin{bmatrix} 0.11554 & 0.07885 \\ 0.07885 & 0.11554 \end{bmatrix}. \tag{19}$$

With multiple coupled interconnects ($\mathbf{L}_{partial}$ in (15) and $\mathbf{C}$ in (18)) converted into two coupled signal lines ($\mathbf{L}_{effective}$ in (16) and $\mathbf{C}_{effective}$ in (19)), an estimate of the crosstalk noise voltage can be made from the analytic equations in [4]. It is shown in [4] that two coupled interconnects can be decoupled into two isolated signal lines, and the peak crosstalk noise occurs at the time of flight, t_f or $3t_f$. Applying the analytic formula in [4] to the effective inductance matrix and effective capacitance matrix in (16) and (19), respectively, with a driver resistance of 50 Ω and a load capacitance of 40 fF, the peak crosstalk noise can be determined. To compare the effective mutual inductance and coupling noise with the simulations, the separation between the two signal lines is varied from 0.6 μm to 3 μm, and the comparisons are shown in Figs. 4 and 5. The analytic solution of the crosstalk noise exhibits an average error of 3.5% as compared to SPICE. An estimate of the crosstalk noise for multiple coupled *RLC* interconnects based on the approach of an effective mutual inductance is, therefore, shown to be both practical and efficient.

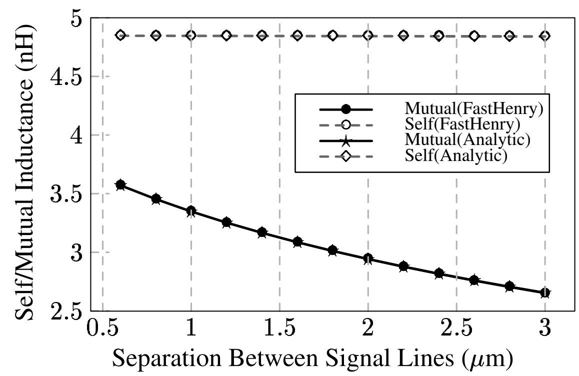

Fig. 4. Comparison of calculated effective loop inductance and effective mutual inductance to the simulation results provided by FastHenry for different separations between the aggressor and victim lines.

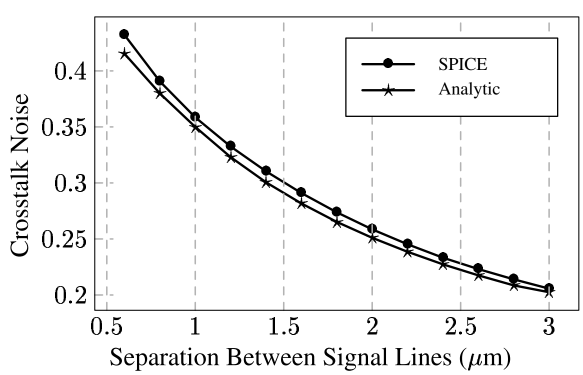

Fig. 5. Comparison of analytic solution of peak crosstalk noise to SPICE for different separations between the aggressor and victim lines.

III. The Effect of Shield Insertion on Reducing Crosstalk Noise

The problem of crosstalk becomes worse as the interconnect exhibit significant inductive effects. A step input asserted at the

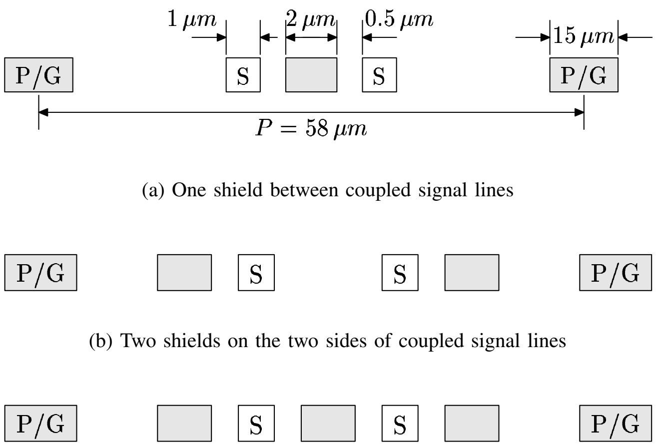

(a) One shield between coupled signal lines

(b) Two shields on the two sides of coupled signal lines

(c) Three shields on both sides of each signal line

Fig. 6. Different structures for inserting shield lines to reduce crosstalk noise

aggressor line, in general, can cause crosstalk noise to oscillate in the victim line. To guarantee signal integrity and reduce delay uncertainty, shield lines are often inserted near the sensitive signal lines. Shield insertion can greatly reduce capacitive coupling [1], while also decreasing the inductive coupling between the signal lines by providing a closer current return path for both the aggressor and victim lines. Far reaching inductive coupling, however, cannot be completely eliminated, producing substantial crosstalk noise on the quiescent victim line.

As shown in Fig. 6, three structures for inserting shield lines are presented. One shield is inserted between the aggressor line and the victim line as shown in Fig. 6(a), two shields are inserted along the two sides of coupled signal lines as illustrated in Fig. 6(b), and three shields are inserted along both sides of each signal line as depicted in Fig. 6(c). An estimate of the crosstalk noise based on the approach of an effective mutual inductance as described in Section II is applied to each of these interconnect structures. The partial inductance matrices are extracted, followed by the determination of the ground return current paths. The effective loop inductance and effective mutual inductance are determined from (9) - (12), and the crosstalk noise is obtained from analytic equations in [4]. SPICE simulations of each of these interconnect structures are compared in Table I to the analytic models. The analytic solution for the peak crosstalk noise exhibits an average error of 12% as compared to SPICE.

TABLE I
EFFECT OF SHIELD INSERTION ON EFFECTIVE MUTUAL INDUCTANCE AND CROSSTALK NOISE

No. of Shields	Effective Inductance (nH)		Crosstalk Noise ($\%V_{dd}$)		
	Mutual	Loop	Analytical	SPICE	Error
No shield	2.655	4.839	20.25%	20.57%	1.56%
One shield	0.086	2.269	4.10%	4.90%	16.32%
Two shields	0.437	2.115	7.18%	5.79%	24.01%
three shields	-0.045	1.634	2.84%	2.67%	6.37%

As shown in Table I, inserting a shield line in the vicinity of a signal line can greatly reduce the effective mutual inductance, significantly reducing the coupling noise. A shield inserted between the aggressor line and the victim line as shown in Fig. 6(a) has a greater effect on reducing the effective mutual inductance than inserting shield lines along the other side of the signal lines as shown in Fig. 6(b). The two shield scenario also does not eliminate the capacitive coupling, which contributes to a higher crosstalk noise than the one shield scenario. The three shield interconnect structure shown in Fig. 6(c) has the least crosstalk noise. This structure, however, requires the highest silicon area. The two shield structure shown in Fig. 6(b) reduces the crosstalk noise to a level comparable with the three shield structure, suggesting that a pattern of a shield line for every two global signal lines is a desirable structure to control crosstalk noise. Another interesting phenomenon is that the effective loop inductance drops with each inserted shield line, reducing the inductance of the signal lines.

IV. Conclusions

Using the equivalence of magnetic energy, an effective mutual inductance is proposed in this paper to efficiently describe the inductive coupling between an aggressor line and a victim line. Based on the effective mutual inductance, the problem of estimating the crosstalk noise among multiple coupled interconnects can be simplified into crosstalk between only two coupled signal lines. Crosstalk noise among multiple coupled *RLC* interconnects, therefore, can be analytically determined, permitting the signal integrity to be efficiently estimated in both the early routing and later verification stages of the IC design process. The concept of an effective mutual inductance is further applied to shield insertion, providing guidelines for inserting shields to reduce crosstalk noise in the presence of both capacitive and inductive coupling. It is shown that a shield line in the vicinity of the signal lines can greatly reduce inductive coupling. A pattern of a shield line for every two global signal lines in the upper metal layers is shown to be desirable for controlling crosstalk noise.

References

[1] J. Zhang and E. G. Friedman, "Crosstalk Noise Model for Shielded Interconnects in VLSI-based Circuits," *Proceedings of the IEEE International SOC Conference*, pp. 243–244, September 2003.
[2] S. P. Sim, S. Krishnan, D. M. Petranovic, D. A. Arora, K. Lee, and C. Y. Yang, "A Unified *RLC* Model for High-Speed On-Chip Interconnects," *IEEE Transactions on Electron Devices*, Vol. 50, No. 6, pp. 1501–1510, June 2003.
[3] P. Saxena and S. Gupta, "On Integrating Power and Signal Routing for Shield Count Minimization in Congested Regions," *IEEE Transactions on Very Large Scale Integration (VLSI) Systems*, Vol. 22, No. 4, pp. 437–445, April 2003.
[4] J. Zhang and E. G. Friedman, "Crosstalk Modeling for Coupled *RLC* Interconnects based on Decoupling Technique," *Proceedings of the IEEE International Symposium on Circuits and Systems*, May 2004.
[5] K. L. Shepard and Z. Tian, "Return-Limited Inductances: A Practical Approach," *IEEE Transactions on Computer-Aided Design of Integrated Circuits and Systems*, Vol. 19, No. 4, pp. 425–436, April 2000.
[6] A. E. Ruehli, "Inductance Calculations in a Complex Integrated Circuit Environment," *IBM Journal of Research and Development*, Vol. 16, No. 5, pp. 470–481, September 1972.
[7] B. Krauter and S. Mehrota, "Layout Based Frequency Dependent Inductance and Resistance Extraction for On-Chip Interconnect Timing Analysis," *Proceedings of the ACM/IEEE Design Automation Conference*, pp. 303–308, June 1998.
[8] M. Kamon, M. J. Tsuk, and J. White, "FASTHENRY: A Multipole-Accelerated 3-D Inductance Extraction Program," *IEEE Transactions on Microwave Theory and Techniques*, Vol. 42, No. 9, pp. 1750–1758, September 1994.
[9] OEA, "NETAN: Multi-Net Three Dimensional Field Solver Extraction Tool User Reference Manual," *OEA international INC.*, 2001.